

C8orf76 promotes gastric tumorigenicity and metastasis by directly inducing lncRNA DUSP5P1 and associates with patient outcomes

Xiaohong Wang^{1,2}, Qiaoyi Liang², Lianhai Zhang¹, Hongyan Gou², Ziyu Li¹, Huarong Chen²,
Yujuan Dong², Jiafu Ji¹, Jun Yu²

¹Key laboratory of Carcinogenesis and Translational Research, Peking University Cancer Hospital and Institute, Beijing, China.

²Institute of Digestive Disease and Department of Medicine and Therapeutics, State Key Laboratory of Digestive Disease, Li Ka Shing Institute of Health Sciences, CUHK-Shenzhen Research Institute, The Chinese University of Hong Kong, Shatin, N.T., Hong Kong, China.

Running title: C8orf76 promotes gastric cancer

Key words: C8orf76; DUSP5P1; MAPK signaling; Gastric cancer

Funding Support: The project was supported by the RGC-GRF Hong Kong (14106415, 14111216, 14163817); Science and Technology Program Grant Shenzhen (JCYJ20170413161534162). Vice-Chancellor's Discretionary Fund CUHK; Shenzhen Virtual University Park Support Scheme to CUHK Shenzhen Research Institute.

Corresponding authors: Professor Jun Yu, Department of Medicine and Therapeutics, Prince of Wales Hospital, The Chinese University of Hong Kong, Shatin, Hong Kong. Tel: 37636099; Fax: (852) 21445330; Email: junyu@cuhk.edu.hk; or Professor Jiafu Ji, Peking University Cancer Hospital and Institute, Beijing, China. Email: jijiafu@hsc.pku.edu.cn.

Conflict of interest: None to declare.

Word count: Abstract 249; Text, 4830 (from introduction to discussion)

Figures: 6

Translational relevance:

C8orf76 amplification is identified in gastric cancer (GC) by genome screening. C8orf76 is up-regulated in 69.74% and 65.71% of two independent cohorts of primary GC patients. C8orf76 DNA copy number amplification was positively associated with its enhanced expression. C8orf76 plays strong oncogenic role in GC through promoting cell proliferation, migration/invasion, tumorigenesis and tumor metastasis. Mechanistically, C8orf76 specifically targets lncRNA DUSP5P1 for its transcriptional induction, thereby activating MAPK/ERK signaling pathway to promote gastric tumorigenesis. Silencing C8orf76 significantly inhibited cell proliferation, xenograft tumor growth, lung and liver metastasis in nude mice, and suppressed the growth of patient-derived organoids. C8orf76 copy number amplification and overexpression serve as new biomarkers for the outcome of GC patients.

Abstract

Objective: We identified for the first time that C8orf76 (chromosome 8 open reading frame 76) is preferentially amplified in gastric cancer (GC). We elucidated its role and clinical significance in gastric carcinogenesis.

Design: The clinical impact of C8orf76 was assessed in 592 GCs. The biological function of C8orf76 was studied *in vitro*, *in vivo* and in GC patient-derived organoid models. C8orf76 downstream effector and pathways were identified by RNA-sequencing, ChIP-sequencing, luciferase reporter and electrophoretic mobility shift assay.

Results: C8orf76 was upregulated in 69.74% and 65.71% of two independent cohorts of GCs and was positively associated with C8orf76 amplification. Multivariate analysis showed that GC patients with C8orf76 amplification (cohort I n=129; cohort II, n=107) or overexpression (n=356) had a significantly shortened survival. C8orf76 significantly promoted GC cell proliferation, cell cycle transformation, migration/invasion, but suppressed cell apoptosis. Silencing C8orf76 expression exerted opposite effects *in vitro*, and significantly inhibited xenograft tumor growth, lung metastasis and liver metastasis in nude mice. Silencing C8orf76 also significantly suppressed the growth of patient-derived organoids. Mechanically, C8orf76 activated MAPK/ERK signaling cascade. C8orf76 directly bound to the promoter region of lncRNA DUSP5P1 with a binding motif of AGGCTG and activated DUSP5P1 transcription. DUSP5P1 induced MAPK/ERK signaling and promoted gastric tumorigenesis. Knockdown DUSP5P1 abrogated the effect of C8orf76 in activating MAPK/ERK cascade and the tumor-promoting function.

Conclusions: C8orf76 directly binds to oncogenic lncRNA DUSP5P1 to induce its expression and activates MAPK signaling. C8orf76 plays pivotal oncogenic role in

gastric carcinogenesis and is an independent prognostic factor for GC patients.

INTRODUCTION

Gastric cancer (GC) is the third leading cause of cancer-related mortality globally^{1, 2}. About half of the GC exhibits chromosomal instability, including gene copy number gain and loss³. Overexpressed oncogenes by copy number gain are involved in GC progression, including HER2, MYC, SRC, EGFR, FGFR1, FGFR2, *et al*⁴⁻⁶. The focal amplification of these gene regions and an increased frequency of their amplification are also associated with invasive clinicopathological characteristics and poor disease prognosis^{4, 5}. However, until now, Trastuzumab is the only approved target agent for a subgroup of GCs with HER2 overexpression⁷. Identification of new factors mediated by gene amplification may provide new insights into the diagnosis and target therapy of GC.

Using human genome comparative genomic hybridization microarray to profile copy number variations in gastric cancer patients⁵, we have previously demonstrated that copy number gain was frequently occurred in chromosomes region 8q22, 8q24, and 20q11-q13, and was significantly associated with poor survival of gastric cancer patients. We identified that C8orf76 (*chromosome 8 open reading frame 76*), a nuclear protein-coding gene, is preferentially amplified in primary GCs as compared to adjacent non-tumor mucosa tissues. The C8orf76 gene is located on chromosome 8q24.13 and encodes a 380-aa protein, a recurrent amplification region in GC⁸. Data in the Human Protein Atlas shows that C8orf76 overexpression is associated with the poor prognosis in renal cancer, endometrial cancer and breast cancer (<https://www.proteinatlas.org/ENSG00000189376-C8orf76/pathology>). We thus speculated that C8orf76 gene amplification is a major mechanism in gastric carcinogenesis through its overexpression. However, the functional significance of

C8orf76 in GC has not yet been explored. In this study, we evaluated the amplification and overexpression status of C8orf76 in GC, characterized the functional mechanisms and the clinical impacts of C8orf76 in gastric carcinogenesis.

MATERIALS AND METHODS

Patients and human samples

Three cohorts of patients with histologically-confirmed GC were included in the study. Cohort I included 129 paired GC tumor tissues and adjacent non-tumor tissues from Peking university cancer hospital, Beijing, China. Cohort II included 107 paired GC tumor tissues and adjacent non-tumor tissues from Prince of Wales Hospital at the Chinese University of Hong Kong, Hong Kong. Cohort III was tissue microarray (TMA) sets covering 356 GC tumor tissues collected at The Prince of Wales Hospital, Hong Kong. In addition, 17 paired paraffin-embedded slides from primary gastric tumor and adjacent non-tumor sites from patients with GC were obtained at the Peking university cancer hospital. The detailed patients' information of three cohorts, were shown in **Figure S1** and **Table S1**. The TNM stage of GC was classified according to the 7th edition of classification recommended by the American Joint Committee on Cancer (AJCC). All subjects provided informed consent for obtaining the study specimens. This study was approved by the Institutional Review Boards of Peking University Cancer Hospital and the Clinical Research Ethics Committee of the Chinese University of Hong Kong. This study was carried out in accordance with the Declaration of Helsinki of the World Medical Association.

Cell lines

Six GC cell lines (AGS, BGC823, MKN74, MGC803, KatoIII, and SNU719) and one normal gastric epithelial cell line GES1 were used in this study. HEK293T, KATOIII and AGS were obtained from ATCC (American Type Culture Collection, Manassas, VA). BGC823, MGC803 and GES1 were obtained from Cell Research Institute, Shanghai, China. MKN74 was obtained from JCRB (Japanese Collection of Research Bioresources Cell Bank, Japan). SNU719 was obtained from KCLB (Korean Cell Line Bank, Seoul, Korea). These cell lines were obtained between 2014 and 2015 and cells authentication were confirmed by short tandem repeat profiling. Cells were cultured in Dulbecco's modified Eagle's medium (Gibco BRL, supplemented with 10% fetal bovine serum (Gibco BRL). Routine Mycoplasma testing was performed by PCR. Cells were grown for no more than 20 passages in total for any experiment.

***In vivo* tumorigenicity and metastasis assays**

BGC823 cells, (2×10^6 cells) stably transfected with shC8orf76 vector, sh-negative control (shNC) vector, DUSP5P1 expression vector or its control vector, were injected subcutaneously into the left and right flanks of 4-week-old male Balb/c nude mice (n=10 per group). Tumor volume (mm^3) was estimated by measuring the longest and shortest diameters of the tumor and calculated as previously described⁹. At the end of experiments, mice were sacrificed and the tumors were weighed and stored for further analyses. To assess the effect of C8orf76 on tumor metastasis, BGC823 cells (2×10^6 cells) stably transfected with shC8orf76 vector or control vector were injected into the tail vein of 6-week-old male Balb/c nude mice (n=10 per group). Four weeks after injection, the mice were sacrificed and examined. The lungs were

dissected and paraffin embedded, and the sections were stained with hematoxylin and eosin (H&E). Metastatic tumors in the lungs were counted in a blinded manner. Liver metastasis GC mouse model was also established. BGC823 cells (1×10^6 cells) stably transfected with shC8orf76 vector or shNC vector were injected into the portal vein of 6-week-old male Balb/c nude mice ($n=5$ per group). Four weeks after injection, the mice were sacrificed and examined. The liver and the celiac implantation tumor including the intestinal tract were dissected and paraffin embedded, and the sections were stained with hematoxylin and eosin (H&E). Metastatic tumors in the livers and abdominal cavity were counted in a blinded manner. All animal experimental procedures were approved by the Animal Ethics Committee of the Chinese University of Hong Kong.

Chromatin immunoprecipitation (ChIP)-sequencing

ChIP assays were done as previously described¹⁰. Briefly, 2×10^7 cells were prepared, crosslinked with 1% formaldehyde, unreacted formaldehyde was quenched with 1 ml of 10x glycine, and then lysed with lysis buffer. Sonication was used to break genomic DNA into small DNA fragments. Anti-FLAG antibody was added and used to immunoprecipitate DNA fragments corresponding to the promoter regions. Input was used as a control. The DNA fragments bound by proteins were then isolated and sequenced using the Illumina HiSeq X-ten platform (Shanghai Biotechnology Co., China). Sequencing raw reads were preprocessed by filtering out sequencing adapters, short-fragment reads and other low-quality reads. Bowtie (version 0.12.8) was then used to map the clean reads to the human hg19 reference genome. Peak detection was performed by MACS (version 1.4.2;

<https://pypi.python.org/pypi/MACS/1.4.2>). The protein-binding motifs were identified using MEME software (<http://meme-suite.org/>).

Patient-derived organoids (PDO) model

The tissues from 3 patients with advanced GC were chopped into pieces and digested. Dissociated cells were collected and seeded with complete human organoid medium. Then the cells were passed on to the 6 wells plate and transfected with C8orf76 siRNA or negative control siRNA (100 nM). After 6 hours, organoids were seeded in 96-well cell culture plates. MALME3 CTG Assay were performed to measure the value in cell-based system using plate reader. This study was approved by the Institutional Review Boards of Peking University Cancer Hospital.

Electrophoretic mobility shift assay

Electrophoretic mobility shift assay (EMSA) and super-shift EMSA gel shifts were conducted as previously described¹¹. Briefly, HEK293T cells were transiently transfected with FLAG-C8orf76 plasmid using Lipofectamine® 2000 Transfection Reagent (Life Technologies, Carlsbad, CA) and 48 hours later nuclear protein extracts were prepared with NE-PER Nuclear and Cytoplasmic Extraction Reagent Kit (Thermo Scientific). Double stranded DNA probes, generated by annealing of sense and antisense oligonucleotides, were biotin-labeled and C8orf76 DNA-binding activity was determined by the LightShift Chemiluminescent electromobility shift assay (Thermo Scientific). For blotting, a Biotinylated nylon membrane (Thermo Scientific) was used. Signals were detected by applying stabilized Streptavidin Horseradish Peroxidase Conjugate and luminol solution (Thermo Scientific). The

sequences of EMSA oligonucleotides and antibodies used are listed in Supporting **Table S2** and **S3** respectively.

RNA-sequencing

The total amount of 3 µg RNA per sample was used as input material for the RNA sample preparations. All samples had RIN values above 6.8. Sequencing libraries were generated using IlluminaTruSeq™ RNA Sample Preparation Kit (Illumina, San Diego, CA), following manufacturer's recommendations. The libraries were sequenced on an Illumina HiSeq X-ten platform as per manufacturer's instructions. (Shanghai Biotechnology Co., China).

Statistical analysis

The results were expressed as mean ± SD. Statistical analysis was performed using the Statistical Package for the Social Sciences (SPSS) (standard V.16.0) (IBM Corporation, New York, USA). The Pearson correlation coefficient was used to evaluate the correlation between C8orf76 gene amplification and expression in the clinical samples. The χ^2 test was used for comparison of patient characteristics and distributions of expression and covariates by vital status. Crude relative risks (RRs) of death associated with C8orf76 expression and other predictor variables were estimated by univariate Cox proportional hazards regression model. Multivariate Cox model was constructed to estimate the adjusted RR for C8orf76 expression. Kaplan–Meier analysis was used to compare the survival distributions of two groups with log-rank test. Mann–Whitney U test or Student's t test was performed to compare the variables of two groups. The difference in cell viability and tumor growth rate

between the two groups was determined by repeated-measures analysis of variance. P value < 0.05 were taken as statistical significance, and all tests were two-tailed.

Other details and additional experimental procedures are provided in Supporting Materials and Methods.

RESULTS

DNA copy number gain contributes to C8orf76 overexpression in primary GC

DNA copy number gain of C8orf76 was identified in 55.81% (72/129) of primary GC patients in cohort I and 58.88% (63/107) in cohort II. Among them, copy number was equal or greater than 3 in 30.23% (39/129) from cohort I and 35.51% (38/107) in cohort II GCs (**Figure 1A**). C8orf76 mRNA expression was significantly increased in 69.74% (53/76, $P<0.0001$) of primary gastric tumors in cohort I, and 65.71% (46/70, $P=0.0116$) in cohort II (**Figure 1B, left panel**) as compared with the paired adjacent non-tumor tissues. In keeping with mRNA expression, C8orf76 protein expression was significantly higher in primary gastric tumors as compared to adjacent non-tumor tissues by immunohistochemical (IHC) staining ($P=0.0006$, **Figure 1C**). In addition, C8orf76 mRNA levels were significantly higher in GCs with copy number amplification ($P<0.0001$ in Cohort I and $P=0.0022$ in Cohort II, **Figure 1D, upper panel**), and C8orf76 mRNA showed positive correlation with its DNA copy number amplification (Cohort I: $R=0.2774$, $P=0.037$; Cohort II: $R=0.3675$, $P<0.0001$, **Figure 1D, lower panel**). Consistently, C8orf76 mRNA overexpression were confirmed in GC patients as compared with the adjacent non-tumor tissues from TCGA datasets (www.cbioportal.org)^{12, 13} ($P<0.0001$, **Figure 1B, right panel**). C8orf76 DNA copy number amplification is also present in GC samples and confirmed a positive association between C8orf76 copy number amplification and its mRNA expression

($R=0.6092$, $P<0.0001$, **Figure 1D, right panel**) from TCGA dataset. These findings demonstrate that DNA copy number gain contributes to upregulation of C8orf76 in GCs.

C8orf76 is a poor prognostic factor in patients with GC

To evaluate the clinical significance of C8orf76 in GC, protein expression of C8orf76 was examined in 356 primary gastric tumor tissues (**Figure 1E**). High C8orf76 protein expression was significantly associated with more advanced tumor stage ($P<0.05$) and diffuse type GC ($P<0.01$) (**Table S4**). High C8orf76 expression predicted a higher risk of cancer-related death by univariate Cox regression analysis (relative risk (RR) =1.882; 95% CI, 1.412-2.510; $P<0.0001$, **Table S5**). Multivariate Cox regression analysis showed that C8orf76 expression was an independent poor prognostic factor for GC patients (RR=1.644; 95% CI, 1.166 - 2.317; $P<0.01$; **Table S6**). As shown in the Kaplan-Meier survival curve, patients with C8orf76 protein expression had significantly shorter survival than those with low or silenced C8orf76 expression ($P<0.0001$, log-rank test) (**Figure 1F**). After stratified by tumor staging, C8orf76 overexpression predicted poor prognosis in stage I-III GC patients, but not for stage IV GC patients (**Figure 1F**).

Moreover, C8orf76 amplification was also associated with advanced tumor stage (Cohort I, $P=0.008$, Cohort II, $P=0.035$, **Table S7**), and poor prognosis of GC patients by univariate Cox regression analysis ($P=0.001$ in Cohort I and II) (**Table S8**) and by multivariate Cox regression analysis (Cohort I: $P=0.013$; Cohort II: $P=0.007$) (**Table S9**). Kaplan-Meier survival analysis demonstrated that C8orf76 amplification predicted shortened survival for GC patients (Cohort I: $n=129$, median 22.3 vs 38.9

months, $P=0.0004$; Cohort II: $n=129$, median not reached vs 19.56 months, $P=0.0004$, log-rank test), especially for stage I-II patients (Cohort I: $P<0.001$; Cohort II: $P=0.0231$; **Figure 1G**). These findings indicate that C8orf76 overexpression/amplification predict poor prognosis in early stage of GC patients.

C8orf76 promotes cell growth and cell cycle progression, but inhibits cell apoptosis

C8orf76 was overexpressed in 4 out of 6 GC cells (NGC823, MGC803, MKN74 and Kato III), weak expressed in AGS and SNU719 cells, but silenced in the normal gastric epithelial cell line GES1 (**Figure 2A**). C8orf76 DNA copy number amplification was identified in BGC823, MGC803, MKN74 and Kato III, but not in AGS and SNU719 (**Table S10**), which was consistent with the expression of C8orf76 in GC cell lines. To investigate the function of C8orf76 in GC, C8orf76 expression vector or empty vector was stably transfected into cells with low C8orf76 expression (AGS and GES1). Ectopic expression of C8orf76 was confirmed by RT-PCR and western blot (**Figure 2B**). The up-regulation of C8orf76 significantly promoted cell viability and clonogenicity in AGS and GES1 (**Figure 2C1**). We next investigated the effect of C8orf76 on cell cycle and apoptosis by flow cytometry. Ectopic expression of C8orf76 expression accelerated G1/S phase progression in AGS and GES1 cells, via upregulation of cyclin D1, cyclin D3 and CDK4, but inhibiting p18 and p53 expression (**Figure 2C2**). In addition, ectopic expression of C8orf76 led to a significant reduction in cell apoptosis at both early and late stage with decreased expression of active (cleaved) forms of caspase-3, caspase-7 and caspase-9 (**Figure 2C3**). Conversely, knockdown of C8orf76 by RNA interference in BGC823 and MKN74 cells (**Figure 2D**) markedly inhibited cell viability and clonogenicity

(**Figure 2E1**), decelerated the G1-S cell cycle transition (**Figure 2E2**) and induced cell apoptosis (**Figure 2E3**). Therefore, C8orf76 promotes cell proliferation in GC through promoting G1-S cell cycle progression but inhibiting apoptosis.

C8orf76 promotes the growth of subcutaneous xenograft tumors in nude mice

To further investigate the tumorigenic ability of C8orf76, we subcutaneously injected BGC823 cells stably transfected with shC8orf76 or a shNC into the left and right dorsal flanks of nude mice, respectively. As shown in **Figure 2F**, knockdown of C8orf76 markedly reduced tumor size ($P<0.0001$) and weight ($P<0.01$) of BGC823 xenografts (**Figure 2F1**). The efficient knockdown of C8orf76 in xenograft tumors was confirmed by immunohistochemistry (**Figure 2F2**). In concordance with the *in vitro* findings, fewer proliferating cells ($P<0.001$) concomitant with more apoptotic cells ($P<0.001$) were detected in BGC823-shC8orf76 xenografts as compared to controls, as demonstrated by Ki-67 and TUNEL assays, respectively (**Figure 2F2**). Our *in vivo* results further support the tumor-promoting role of C8orf76 in GC.

C8orf76 promotes migration and invasion of GC cells

Ectopic expression of C8orf76 promoted the cell migration and invasions in AGS and GES1 cells by wound healing assay and Matrigel invasion assays (both $P<0.01$; **Figure 3A, B**), respectively. Conversely, C8orf76 knockdown in BGC823 and MKN74 cells exerted opposite effects (both $P<0.01$; **Figure 3A, B**). Ectopic expression of C8orf76 promoted the epithelial-mesenchymal transition (EMT) through up-regulation of mesenchymal markers (N-cadherin, β -catenin, Slug and Vimentin) and down-regulation of epithelial markers (E-cadherin), as shown by immunocytostaining. In contrast, silencing of C8orf76 showed the opposite effect on

these EMT markers (**Figure 3C, Figure S2**). These results demonstrate that C8orf76 plays an important role in promoting the invasiveness of GC cells.

C8orf76 promotes GC metastasis to lung and liver *in vivo*

We further assessed the effect of C8orf76 on tumor metastasis *in vivo*. The BGC823 cells stably transfected with shC8orf76 or shNC were injected through tail vein of nude mice. After four weeks, histological examinations demonstrated that 80% (8/10) of the mice bearing BGC823-shNC cells exhibited lung metastases, while only 20% (2/10) of the mice bearing BGC823-shC8orf76 showed lung metastases ($P<0.05$, **Figure 3D**). Moreover, the number of metastatic lesions was significantly fewer in shC8orf76 group than in control group ($P<0.001$).

To confirm the effect of C8orf76 in promoting metastasis, we inoculated nude mice with a single administration of BGC823 cells stably transfected with shC8orf76 or shNC via portal vein. At the end of experiment, significantly fewer tumor nodules on the peritoneal surfaces in shC8orf76 group were observed as compared to control group ($P<0.05$, **Figure 3E, upper panel**). Histological examination showed that average number of metastatic lesions in liver from shC8orf76 group was also significantly fewer as compared to control group ($P<0.05$, **Figure 3E, lower panel**). Collectively, these results indicate the important role of C8orf76 in promoting GC metastasis.

C8orf76 is a potential target in patient-derived GC organoid model

To investigate if C8orf76 could be a potential target for GC, we established personalized PDO models, which were generated from three advanced GC cases

with different clinicopathological features (**Figure 3F, Table S11**). As shown in **Figure 3F**, knockdown of C8orf76 significantly suppressed the GC cell growth in three PDO models. Our findings suggest that C8orf76 may serve as a potential target in GC patients.

5-Fu treatment decreased the expression of C8orf76

We examined the possibility that chemotherapy affects the expression of C8orf76 in gastric cell lines, AGS and GES1 cells stably transfected with C8orf76 are treated with 5-Fu at 5 μ mol and 10 μ mol respectively for 24 hours. We found that the mRNA and protein expression of C8orf76 is significantly reduced after exposure to 5-Fu in both AGS and GES1 cells. (Figure 3G, $P < 0.01$).

C8orf76 induces MAPK/ERK signaling cascade

To further understand the molecular mechanisms underlying pro-tumorigenic action of C8orf76, gene expression profiles were analyzed by RNA-sequencing in C8orf76-knockdown cell lines BGC823 and MKN74 compared with their control counterparts. KEGG pathway enrichment analysis was performed on the differentially expressed genes detected in both BGC823 and MKN74. The result showed that C8orf76 knockdown significantly dysregulated MAPK signaling, cell cycle, p53 signaling, Wnt signaling, TGF-beta signaling, apoptosis and ErbB signaling pathways (**Figure 4A**). Among them, MAPK signaling was the most enriched pathway. Silencing C8orf76 inhibited MAPK activities in both BGC823 and MKN74 cells as demonstrated by luciferase reporter assay (**Figure 4B**). Consistently, IHC staining showed the reduction of the protein expression of several key MAPK signaling genes including p-ERK1/2, p-p38 and p-c-Jun in xenograft tumors with C8orf76 knockdown as

compared to control group (**Figure 4C**). On the contrary, ectopic expression of C8orf76 significantly increased MAPK activities in AGS and GES1 cells (**Figure 4D**), accompanied with increased protein expression of p-ERK1/2, p-p38, p-JNK and p-c-Jun (**Figure 4D**). We then tested whether the MAPK pathway inhibitors could blunt the tumor-promoting effect of C8orf76. As shown in **Figure 4E**, treatment with ERK inhibitor significantly suppressed ERK activity, MAPK signaling, and abolished the promoting effect of C8orf76 on the cell growth in both AGS and GES1 (**Figure 4E1**). Consistent results were obtained by using other MAPK pathway inhibitors such as p38, c-jun inhibitor (**Figure 4E2, E3**). Therefore, C8orf76 exerts the tumor-promoting effect by activating MAPK/ERK signaling.

lncRNA DUSP5P1 (dual specificity phosphatase 5 pseudogene 1) is a direct downstream target of C8orf76

We next analyzed the protein structure and cellular localization using PredictProtein (<https://www.predictprotein.org>). Results showed that C8orf76, a potential transcription factor with a zinc finger structure, mainly localizes in nucleus (**Figure 5A**). The nuclear localization of C8orf76 was validated by western blotting and immunofluorescence staining in both AGS and GES1 cells transfected with C8orf76-vector (**Figure 5A**). **To identify the role of C8orf76 as a transcription factor and its binding sites, ChIP-seq was performed in GES1 cells transfected with C8orf76-vector or control vector. The results revealed 520 C8orf76-binding DNA candidates (Table S12). Of them, 25 candidate genes were identified with binding peaks located at promoter regions (within ±2kb of transcription start site). Motif analysis was then conducted using the MEME online motif comment tool to discover binding motifs. Five typical NFAT 'core' binding motifs were identified, including**

C8orf76 to the AGGCTG motif in the DUSP5P1 promoter was further validated by EMSA (**Figure 5F**). In contrast, no super-shifted band was produced upon “AGGCTG” deletion. **These results demonstrate that C8orf76 directly binds to the “AGGCTG” motif in the promoter of DUSP5P1 and upregulates its transcription (Figure 5F).**

DUSP5P1 promotes GC cell growth *in vitro* and *in vivo*

Ectopic expressing DUSP5P1 in BGC823 and MGC803 cells with low endogenous DUSP5P1 expression significantly increased cell growth and colony formation (**Figure S4A**). Upregulation of DUSP5P1 also significantly increased G1 to S phase cell cycle transition, but decreased early and late apoptotic cells in both MGC803 and BGC823 (**Figure S4A**). Conversely, knockdown of DUSP5P1 in MKN74 and AGS cells showed opposite effects (**Figure S4B**). The tumor promoting effect of DUSP5P1 was further confirmed in subcutaneous xenograft tumor models *in vivo* (**Figure 6A**). Significantly more proliferating cells and fewer apoptotic cells were shown in DUSP5P1-transfected xenografts as compared to control group by Ki-67 and TUNEL assays (both $P < 0.01$; **Figure 6B**), respectively. **These findings collectively confirm the tumor-promoting role of DUSP5P1 in GC.**

The tumor-promoting function of C8orf76 is depending on DUSP5P1

We then assessed whether the tumor-promoting function of C8orf76 in GC depend on DUSP5P1. The results showed that knockdown of DUSP5P1 by siRNA in both AGS and GES1 cells significantly blunted the promoting effects of C8orf76 on cell growth (**Figure 6C**) and colony formation ability (**Figure 6D**), inferring that the tumor-promoting effect of C8orf76 is at least in part depending on DUSP5P1 in GC.

Meanwhile, knockdown of DUSP5P1 significantly diminished C8orf76-mediated MAPK signaling activation (**Figure 6E**) and the protein expression of p-p38, p-c-Jun, p-JNK and p-ERK1/2 (**Figure 6F**), as evidenced by luciferase reporter assays and Western blot, respectively. Further luciferase assay showed that DUSP5P1 overexpression increased MAPK activities in BGC823 and MGC803 cells, while DUSP5P1 knockdown decreased MAPK activities in AGS and MKN74 cells (**Figure 6G**). Moreover, DUSP5P1 overexpression significantly increased the protein expression of p-ERK1/2, p-p38 and p-c-Jun in xenograft tumors by IHC staining (**Figure 6H**). These results collectively indicate that activation of MAPK/ERK signaling by C8orf76 is, at least in part, depending on DUSP5P1 in GC.

DISCUSSION

In this study, we demonstrated that amplification of C8orf76 was detected in 55.8% (cohort I) and 58.88% (cohort II) of primary GCs. Gene amplification is thought to promote over-expression of genes favoring tumor development. We revealed that the amplification of C8orf76 was positively associated with its overexpression in our two cohorts of GC patients and also in TCGA cohort of GC patients, suggesting that increased C8orf76 copy-number contributes to the upregulation of C8orf76 in gastric carcinogenesis. We further evaluated the association of C8orf76 amplification and overexpression with prognosis of GC patients. Both C8orf76 gene amplification and protein overexpression are associated with poor prognosis of GC patients independent of their clinicalpathological features, especially for early stages of GC patients, implying that C8orf76 is an independent prognostic factor of early stage GC patients.

A series of *in vitro* and *in vivo* bio-functional experiments were performed and revealed that C8orf76 possesses strong tumor-promoting function in GC by inducing cell proliferation, G1 to S phase transition and suppressing cell apoptosis *in vitro*; and by promoting the tumorigenesis in nude mice *in vivo*. These results suggested the tumor-promoting role of C8orf76 in GC, and prompted us to address the underlying mechanism by which C8orf76 regulating GC progression. We demonstrated that C8orf76 facilitated the G1-S phase transition by upregulation of the protein expression of critical cell cycle regulators, and the downregulation of key CDK inhibitor p18, which upregulates p53 via interactions with ATM/ATR¹⁵ (Figure 2). Concomitantly with the promotion of cell proliferation, the growth-promoted effect of C8orf76 was also related to the inhibition of apoptosis, as evidenced in the C8orf76-expressing GC cell lines and in xenografted tumors in the nude mice. Therefore, C8orf76 exerts its tumor-promoting effect by regulating cell cycle and cell death to promote tumor growth. In addition to the tumorigenic roles, C8orf76 also promotes GC cell migration and invasion properties *in vitro*. In a tail vein injection mouse model of cancer metastasis, depletion of C8orf76 by shRNA in BGC823 cells significantly inhibited lung metastasis *in vivo*. Consistent with this finding, depletion of C8orf76 in BGC823 cells suppressed liver metastasis by portal vein injection of BGC823 cells in mice. These results further confirm the solid tumor-promoting effect of C8orf76 in gastric carcinogenesis.

We thus considered whether C8orf76 could regulate the cell growth of PDO models generated from GC patients. We found that C8orf76 knockdown significantly suppressed the growth of all three PDO models from three GC patients.

The molecular mechanisms by which C8orf76 exerts its pro-tumorigenesis and pro-metastases functions in GC were evaluated by RNA-sequencing in C8orf76 knockdown and control GC cells. C8orf76 significantly caused dysregulation of signaling pathways including MAPK, cell cycle, p53 signaling, Wnt signaling, TGF-beta signaling, apoptosis and ErbB. As the dysregulated genes mediated by C8orf76 were mainly enriched in MAPK signaling pathway, we validated this pathway *in vitro* and *in vivo*. We confirmed the significantly induced activation of MAPK, in concomitant with enhanced protein expression of key MAPK signaling factors ERK, P38, JNK and c-Jun. In particular, inhibiting MAPK signaling by ERK inhibitor significantly blunted the tumor-promoting role of C8orf76 in GC cells. It is thus, C8orf76 plays an important tumor promoting role in gastric carcinogenesis through dysregulated oncogenic signaling pathways^{16, 17}, especially MAPK/ERK signaling.

After confirmed its nucleus localization of C8orf76, the integrated ChIP-sequencing and RNA-sequencing analyses showed that lncRNA DUSP5P1 is one of the critical downstream targets of C8orf76. The direct binding of C8orf76 to the promoter of DUSP5P1 was demonstrated, and the binding motif (AGGCTG) at the promoter of DUSP5P1 was confirmed by ChIP-PCR and EMSA. C8orf76 actively increased the transcriptional activity and expression of DUSP5P1. As a lncRNA, DUSP5P1 is a pseudogene of DUSP5. The DUSP5/DUSP5P1 system could be responsible for regulation of BCL2L11 leading to the inhibition of apoptosis in HL cells¹⁸. High expression of DUSP5P1 is identified in high-risk AML patients and is associated with poor prognosis in AML¹⁴. The role of DUSP5P1 in tumorigenesis remains unclear. We then performed experiments to study the functional role of DUSP5P1 in GC. Using gain and loss of DUSP5P1 function experiments, we demonstrated that

DUSP5P1 promoted GC tumorigenesis through inducing cell proliferation, G1 to S phase cell cycle transition and inhibiting apoptosis. Particularly, DUSP5P1 knockdown by siRNA significantly abolished the cell growth promoting effect by C8orf76. It is thus, **lncRNA DUSP5P1 is an important direct downstream effector of C8orf76 and the tumor-promoting effect of C8orf76 is partially depending on DUSP5P1 in GC.**

The dual-specificity phosphatases (DUSPs), also known as MAPK phosphatases (MKPs), **are a family of proteins that function as major negative regulators of MAPK activities in mammalian cells¹⁹⁻²¹. We found an inverse correlation between DUSP5P1 (the pseudogene of DUSP5) and DUSPs, including DUSP5 (Table S13).** Pseudogenes serve as the raw and processed materials for the exaptation of novel functions, particularly in relation to the regulation of parental gene expression²². **We thus investigated if C8orf76-mediated activation of MAPK/ERK signaling is depending on DUSP5P1.** As expected, DUSP5P1 knockdown significantly blunted C8orf76 induced activation of MAPK/ERK signaling *in vitro* and *in vivo*, suggesting that **as a direct downstream target of C8orf76, DUSP5P1 plays a pivotal role in C8orf76 mediated activation of MAPK/ERK signaling in gastric tumorigenesis.**

We further demonstrated that DUSP5P1 induced cell proliferation, G1 to S phase transition and suppressed cell apoptosis *in vitro*; and promoted the tumorigenesis in nude mice *in vivo*. **These results addressed the underlying mechanism by which C8orf76 regulating the expression of DUSP5P1 and further promoting GC progression.**

In conclusion, our study reported for the first time that **C8orf76 is a novel tumor-promoting factor in GC by inducing cell proliferation, cell cycle transition, metastasis and inhibiting apoptosis. The mechanisms of C8orf76 as a tumor-promoting factor was mediated by inducing tumor promoting lncRNA DUSP5P1 through directly binding to DUSP5P1 promoter and activating MAPK/ERK signaling pathway (Figure 6I). C8orf76 may serve as a potential prognostic biomarker for the poor outcome of GC patients.**

References

1. Wang K, Liang Q, Li X, et al. MDGA2 is a novel tumour suppressor cooperating with DMAP1 in gastric cancer and is associated with disease outcome. *Gut* 2016;65:1619-31.
2. Jemal A, Bray F, Center MM, et al. Global cancer statistics. *CA Cancer J Clin* 2011;61:69-90.
3. Cancer Genome Atlas Research N. Comprehensive molecular characterization of gastric adenocarcinoma. *Nature* 2014;513:202-9.
4. Gomez-Martin C, Plaza JC, Pazo-Cid R, et al. Level of HER2 gene amplification predicts response and overall survival in HER2-positive advanced gastric cancer treated with trastuzumab. *J Clin Oncol* 2013;31:4445-52.
5. Wang X, Liu Y, Shao D, et al. Recurrent amplification of MYC and TNFRSF11B in 8q24 is associated with poor survival in patients with gastric cancer. *Gastric Cancer* 2016;19:116-27.
6. Stahl P, Seeschaaf C, Lebok P, et al. Heterogeneity of amplification of HER2, EGFR, CCND1 and MYC in gastric cancer. *BMC Gastroenterol* 2015;15:7.

7. Bang YJ, Van Cutsem E, Feyereislova A, et al. Trastuzumab in combination with chemotherapy versus chemotherapy alone for treatment of HER2-positive advanced gastric or gastro-oesophageal junction cancer (ToGA): a phase 3, open-label, randomised controlled trial. *Lancet* 2010;376:687-97.
8. Jin DH, Park SE, Lee J, et al. Copy Number Gains at 8q24 and 20q11-q13 in Gastric Cancer Are More Common in Intestinal-Type than Diffuse-Type. *PLoS One* 2015;10:e0137657.
9. Yu J, Cheng YY, Tao Q, et al. Methylation of protocadherin 10, a novel tumor suppressor, is associated with poor prognosis in patients with gastric cancer. *Gastroenterology* 2009;136:640-51 e1.
10. Casimiro MC, Crosariol M, Loro E, et al. ChIP sequencing of cyclin D1 reveals a transcriptional role in chromosomal instability in mice. *J Clin Invest* 2012;122:833-43.
11. Dorn T, Goedel A, Lam JT, et al. Direct nkx2-5 transcriptional repression of *isl1* controls cardiomyocyte subtype identity. *Stem Cells* 2015;33:1113-29.
12. Cerami E, Gao J, Dogrusoz U, et al. The cBio cancer genomics portal: an open platform for exploring multidimensional cancer genomics data. *Cancer Discov* 2012;2:401-4.
13. Gao J, Aksoy BA, Dogrusoz U, et al. Integrative analysis of complex cancer genomics and clinical profiles using the cBioPortal. *Sci Signal* 2013;6:pl1.
14. Zhou LY, Yin JY, Tang Q, et al. High expression of dual-specificity phosphatase 5 pseudogene 1 (*DUSP5P1*) is associated with poor prognosis in acute myeloid leukemia. *Int J Clin Exp Pathol* 2015;8:16073-80.
15. Park BJ, Kang JW, Lee SW, et al. The haploinsufficient tumor suppressor p18 upregulates p53 via interactions with ATM/ATR. *Cell* 2005;120:209-21.

16. Yang M, Huang CZ. Mitogen-activated protein kinase signaling pathway and invasion and metastasis of gastric cancer. *World J Gastroenterol* 2015;21:11673-9.
17. Kanai M, Konda Y, Nakajima T, et al. Differentiation-inducing factor-1 (DIF-1) inhibits STAT3 activity involved in gastric cancer cell proliferation via MEK-ERK-dependent pathway. *Oncogene* 2003;22:548-54.
18. Staeger MS, Muller K, Kewitz S, et al. Expression of dual-specificity phosphatase 5 pseudogene 1 (DUSP5P1) in tumor cells. *PLoS One* 2014;9:e89577.
19. Nunes-Xavier CE, Tarrega C, Cejudo-Marin R, et al. Differential up-regulation of MAP kinase phosphatases MKP3/DUSP6 and DUSP5 by Ets2 and c-Jun converge in the control of the growth arrest versus proliferation response of MCF-7 breast cancer cells to phorbol ester. *J Biol Chem* 2010;285:26417-30.
20. Patterson KI, Brummer T, O'Brien PM, et al. Dual-specificity phosphatases: critical regulators with diverse cellular targets. *Biochem J* 2009;418:475-89.
21. Bermudez O, Pages G, Gimond C. The dual-specificity MAP kinase phosphatases: critical roles in development and cancer. *Am J Physiol Cell Physiol* 2010;299:C189-202.
22. Thomas C Roberts KVM. Not so pseudo anymore: pseudogenes as therapeutic targets. *Pharmacogenomics* 2014;14:2023-2034.

Figure Legends:

Figure 1. Amplification and upregulation of C8orf76 in primary gastric cancers are associated with poor prognosis of gastric cancer patients. (A) C8orf76 DNA copy number status was examined in 129 GC tissues (cohort I) and 107 GC tissues (cohort II). C8orf76 was frequently gained in GC. **(B)** C8orf76 mRNA expression was significantly upregulated in gastric tumors compared to adjacent non-tumor tissues in Chinese cohort and TCGA cohort. **(C)** Representative images of IHC staining of C8orf76 in GC tumor and adjacent normal tissues. The level of C8orf76 nuclear expression was significantly higher in GC tumor tissues as compared to their adjacent normal tissues by IHC. **(D)** C8orf76 mRNA expression was higher in C8orf76 DNA copy number amplification group compared with no amplification group (upper panel). C8orf76 copy number was positively correlated with its mRNA expression (lower panel). **(E)** Representative images of IHC staining of C8orf76 negative/low and positive staining by IHC. **(F)** Kaplan–Meier survival analysis in GC patients with different C8orf76 protein expression status. **(G)** Kaplan–Meier survival analysis in GC patients with different C8orf76 copy number in cohort I and II. Amp: Amplification (copy number is equal or greater than 3 in cohort I and II).

Figure 2. Role of C8orf76 in GC cells. (A) C8orf76 was highly expressed in GC cell lines but not in the normal gastric cell line GES-1 by RT-PCR and immunocytochemistry. **(B)** Ectopic expression of C8orf76 in AGS and GES1 cells was confirmed by RT-PCR and Western blot. **(C)** C8orf76 expression significantly increased cell viability and clonogenicity **(C1)**, significantly promoted cell cycle G1-S transition, accompanied by enhanced protein levels of CDK4, cyclin-D1 and cyclin-D3, and reduced p18 and p53 **(C2)**, while inhibited cell apoptosis in GES1 and AGS cells, accompanied by reduced levels of the active forms of caspase-7, caspase-9

and caspase-3 **(C3)** in AGS and GES-1 cells. **(D)** Knockdown of C8orf76 by siC8orf76 in BGC823 and MKN74 cells was confirmed by RT-PCR and Western blot. **(E)** C8orf76 knockdown significantly inhibited cell growth and colony formation **(E1)**, caused G1-S arrest **(E2)** and promoted cell apoptosis **(E3)**. **(F)** C8orf76 knockdown inhibited subcutaneous tumorigenicity *in vivo*. **(F1)** Representative images of tumor growth in nude mice subcutaneously inoculated with shC8orf76- or shNC-transfected BGC823 cells were shown. C8orf76 knockdown inhibited subcutaneous tumorigenicity *in vivo* as shown by growth curve of tumor volume, and tumor volume and weight at the end of the experiment. Data were expressed as means \pm SD, n = 10/group. **(F2)** C8orf76 protein expression, cell proliferative activity and cell apoptosis in subcutaneous xenografts were determined by immunohistochemistry, Ki-67 staining and TUNEL staining, respectively.

Figure 3. C8orf76 promotes GC cell migration, invasion in vitro and metastasis in vivo. **(A)** Representative images of wound healing assay revealed that ectopic expression of C8orf76 promoted cell migration in AGS and GES1 cells **(A1)**, while knockdown of C8orf76 inhibited cell migration in MKN74 and BGC823 cells **(A2)**. **(B)** Representative images of matrigel invasion transwell assay revealed that ectopic expression of C8orf76 promoted cell invasion in AGS and GES1 cells **(B1)**, while knockdown of C8orf76 inhibited cell invasion in MKN74 and BGC823 cells **(B2)**. Data was expressed as mean \pm S.D. Student's t-test was performed. **(C)** Representative images of immunostaining of EMT markers in control and ectopic expression of C8orf76 AGS and GES1 cells. C8orf76 expression increased the levels of N-cadherin, β -catenin, Slug and Vimentin, and decreased E-cadherin level in C8orf76-overexpressing cells as indicated by immunostaining, while knockdown of C8orf76 showed the opposite effect on these EMT markers. **(D)** Representative macroscopic

appearances of lung metastasis and HE stained images of the lungs were shown. Silencing of C8orf76 in BGC823 cells significantly reduced the number of metastatic lesions in the lungs (n = 10/group). **(E)** Representative macroscopic appearances of peritoneal surfaces implanting and HE stained images were shown (upper panel). Representative macroscopic appearances of liver metastasis and HE stained images of the liver were shown (lower panel). Silencing of C8orf76 in BGC823 cells significantly reduced the number of metastatic lesions in the peritoneal surfaces and liver (n = 5/group). **(F)** PDOs assay showed C8orf76 knockdown inhibited GC cell growth significantly. The HE staining image (upper panel). Phase-contrast images of PDOs derived from three biopsy core (middle panel). Cell viability was measured in cell-based system using plate reader (lower panel). Data shown are mean \pm SD. **(G)** 5-Fu decreased the expression of C8orf76 both in the RNA and protein levels.

Figure 4. C8orf76 activates MAPK signaling pathway. (A) KEGG pathways enriched by differentially expressed genes affected by C8orf76. **(B)** C8orf76 knockdown inhibited MAPK pathway as evidenced by decreased SRE luciferase activity and protein expression of MAPK signaling pathway in C8orf76 knockdown xenograft tumor tissues **(C)**. **(D)** C8orf76 re-overexpression promoted MAPK pathway as evidenced by increased SRE luciferase activity and protein expression of factors in MAPK signaling pathway in AGS and GES1 cells by Western blot. **(E)** Effect of C8orf76 on gastric cell growth in the presence or absence of MAPK inhibitor. **(E1)** Effect of C8orf76 on gastric cell growth in the presence or absence of ERK inhibitor (GES1, 20 μ mol/L; AGS, 40 μ mol/L). **(E2)** Effect of C8orf76 on gastric cell growth in the presence or absence of p38 inhibitor (GES1, 20 μ mol/L; AGS, 20 μ mol/L). **(E3)** Effect of C8orf76 on gastric cell growth in the presence or absence of c-Jun inhibitor (GES1, 20 μ mol/L; AGS, 20 μ mol/L). Cell growth was measured by

MTT assay. Data shown are mean \pm SD.

Figure 5. DUSP5P1 is a direct downstream target of C8orf76. (A) Nuclear localization of C8orf76 in AGS and GES1 cells following C8orf76 transfection by online prediction, immunofluorescence staining and western blot. **(B)** Flow chart of ChIP-sequencing assay and RNA-sequencing data analysis of transcription factor binding site for C8orf76 to select the direct downstream target genes of C8orf76. **(C)** ChIP-PCR was performed to determine the interaction between C8orf76 and promoter of the downstream genes. **(D)** C8orf76 mRNA expression was correlated with the DUSP5P1 expression. Ectopic expression of C8orf76 increased the mRNA expression of DUSP5P1 in AGS and GES1 by Q-RT-PCR, whilst C8orf76 knockdown decreased the expression of DUSP5P1 (upper panel). C8orf76 mRNA expression was positively correlated with the expression of DUSP5P1 in both cohorts I and II (lower panel). **(E)** Luciferase reporter assay showed that C8orf76 binds to the “AGGCTG” motif. **(F)** EMSA was performed to detect the directly interaction of C8orf76 and the promoter of DUSP5P1.

Figure 6. C8orf76 exerts tumor-promoting function partially depending on the tumor-promoting lncRNA DUSP5P1. (A) Representative images of tumor growth in nude mice subcutaneously inoculated with DUSP5P1 or control vector transfected BGC823 cells were shown. DUSP5P1 expression significantly inhibited subcutaneous tumorigenicity as shown by growth curve of tumor volume, as well as tumor weight at the end of the experiment. Data were expressed as means \pm SD, n = 10/group. **(B)** DUSP5P1 expression, cell proliferative activity and cell apoptosis in xenografts were assessed by RT-(q)PCR, Ki-67 staining and TUNEL staining, respectively. **(C)** Knockdown of DUSP5P1 significantly blunted the promoting effects of C8orf76 on cell growth. Successful knockdown of DUSP5P1 in C8orf76-

overexpressed cells was confirmed by RT-PCR (left panel). Effect of C8orf76 on cell viability with or without DUSP5P1 knockdown by MTT assay were detected. Data are means \pm SD. *** $P < 0.001$ (right panel). **(D)** Effect of C8orf76 on colony formation ability with or without DUSP5P1 knockdown were investigated. DUSP5P1 knockdown partially abolished the tumor-promoting function of C8orf76. **(E)** Effect of C8orf76 on MAPK pathway with or without DUSP5P1 knockdown was detected by SRE luciferase reporter assay. **(F)** Protein expression of factors in MAPK signaling pathway in C8orf76 stable expressing AGS and GES1 cells with transient knockdown of DUSP5P1 by siDUSP5P1 for 48 hours. DUSP5P1 knockdown partially abolished the C8orf76-mediated activation of MAPK signaling. **(G)** DUSP5P1 activated MAPK signaling as evidenced by SRE luciferase reporter assay. **(H)** Protein expression of MAPK signaling pathway in DUSP5P1 overexpression xenograft tumor tissues. DUSP5P1 overexpression increased the activation of MAPK signaling. **(I)** Proposed mechanistic scheme of C8orf76 promoting the MAPK signaling pathway in GC. C8orf76 promoted the expression of DUSP5P1 by directly binding to its promoter, which further promotes the activity of MAPK signaling pathway.

Figure 1

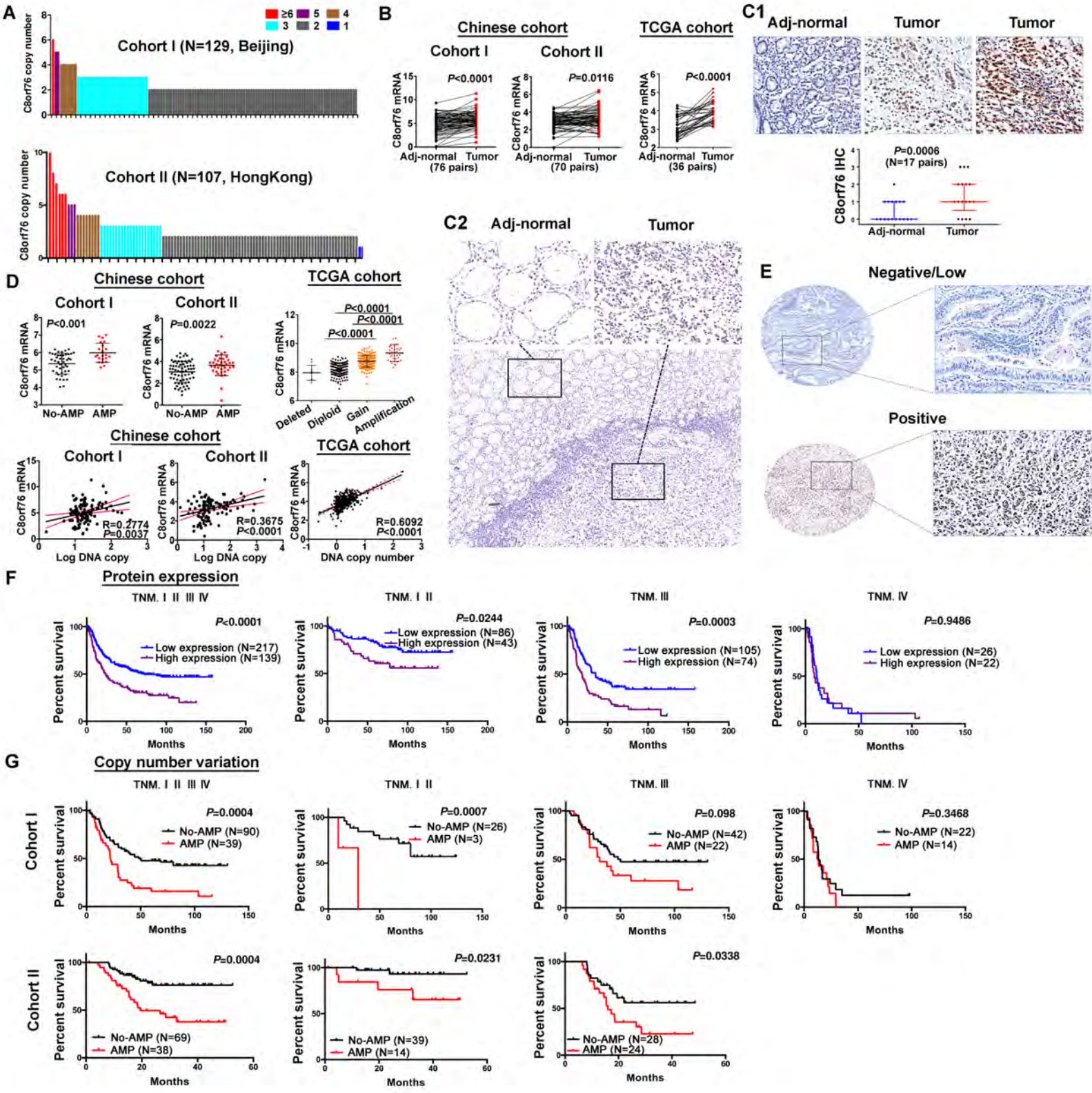


Figure 2

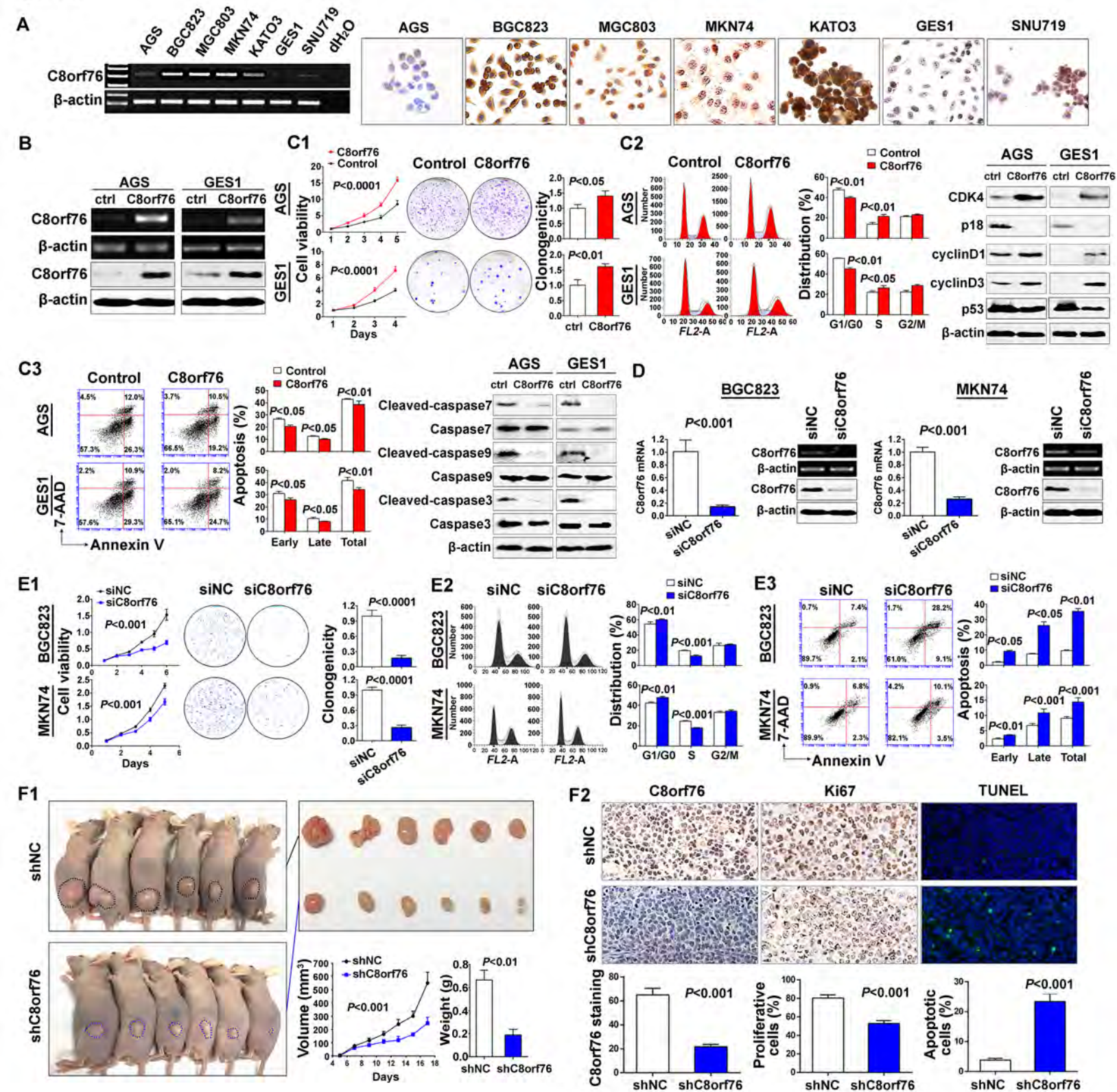


Figure 3

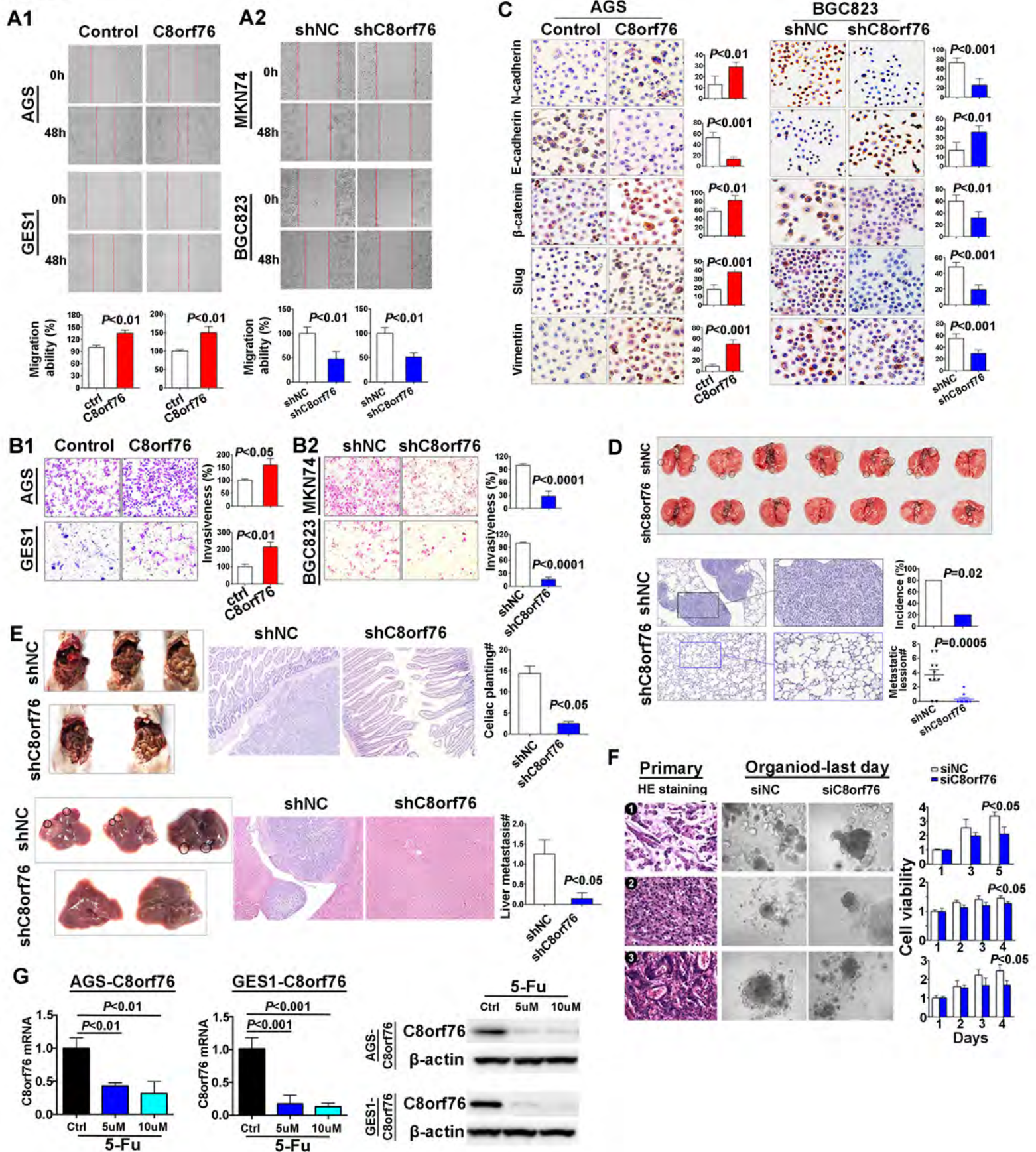


Figure 4

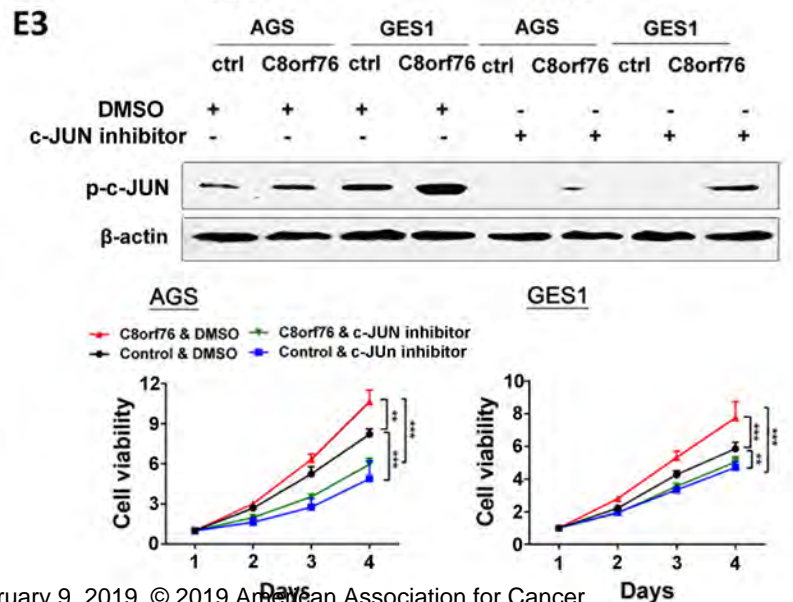
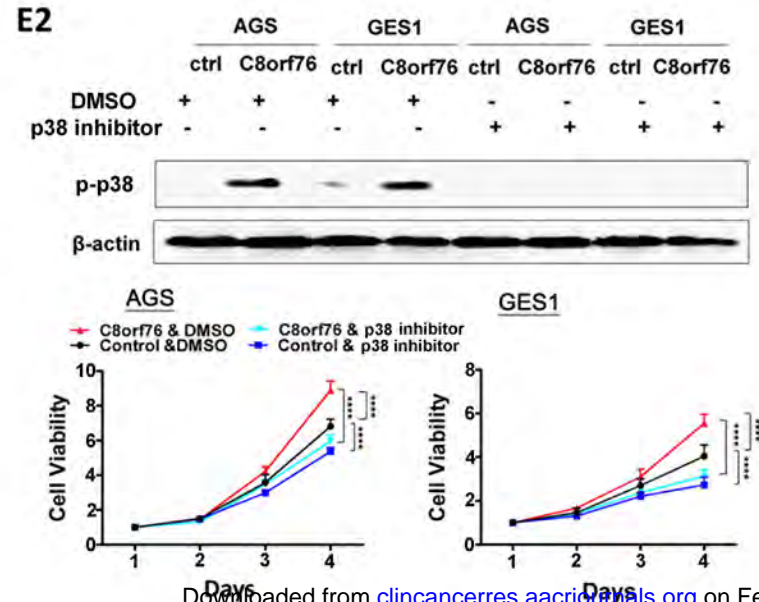
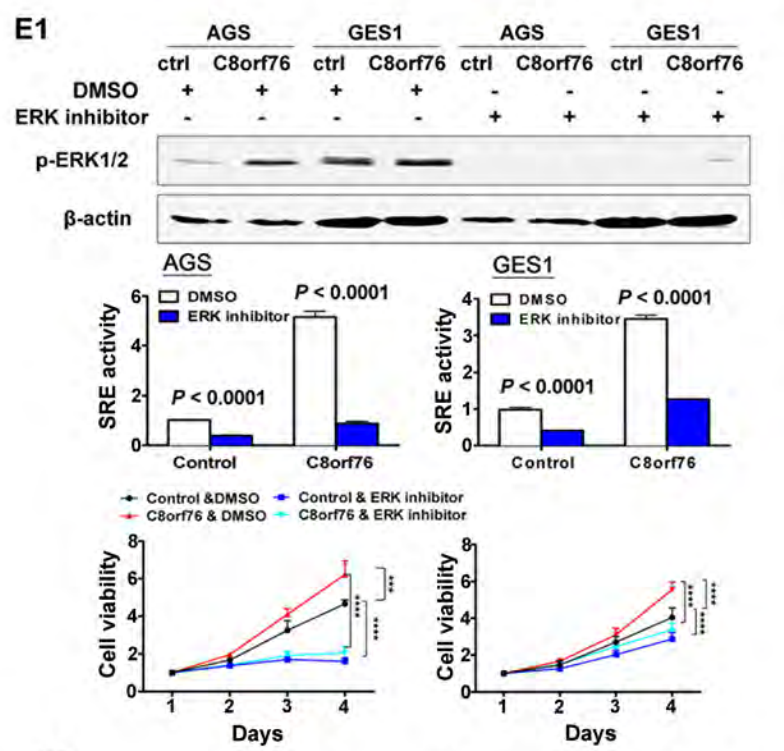
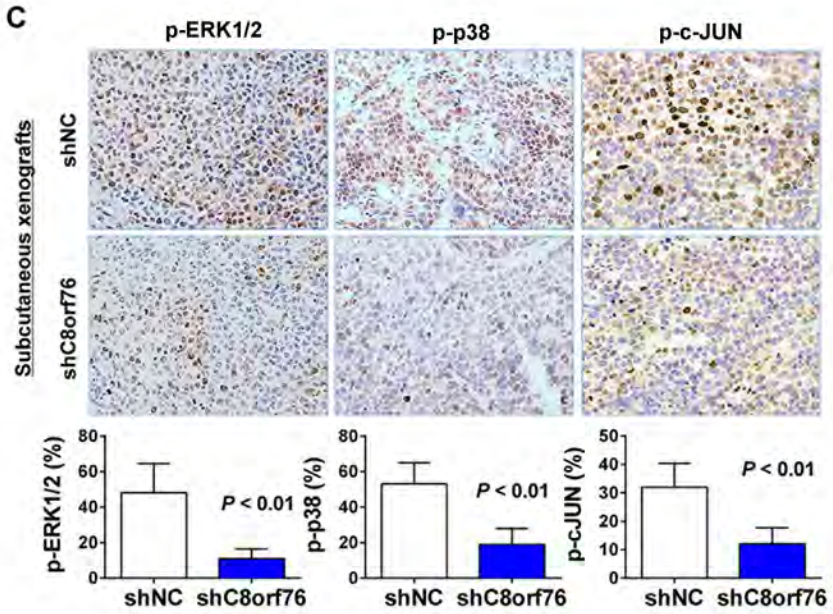
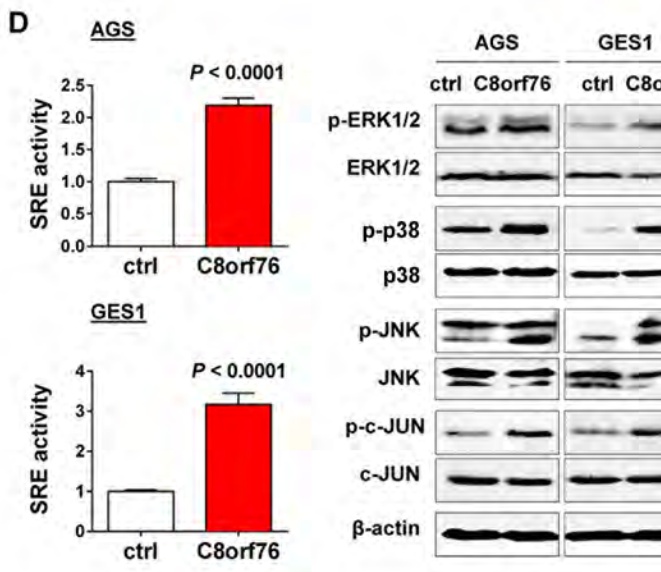
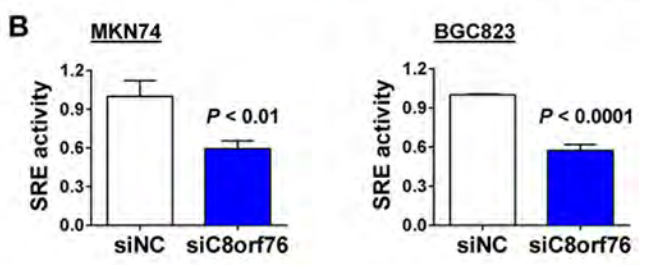
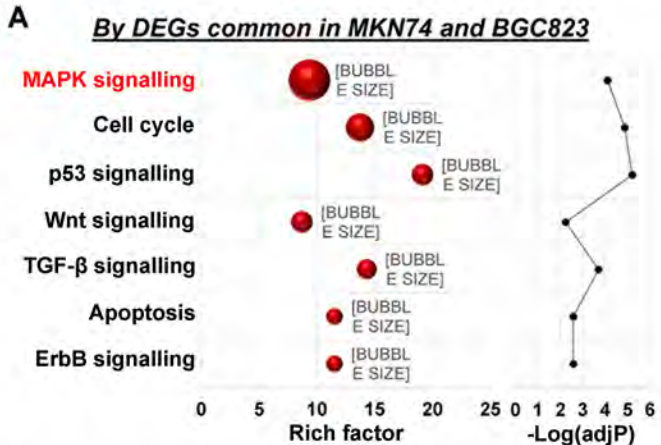
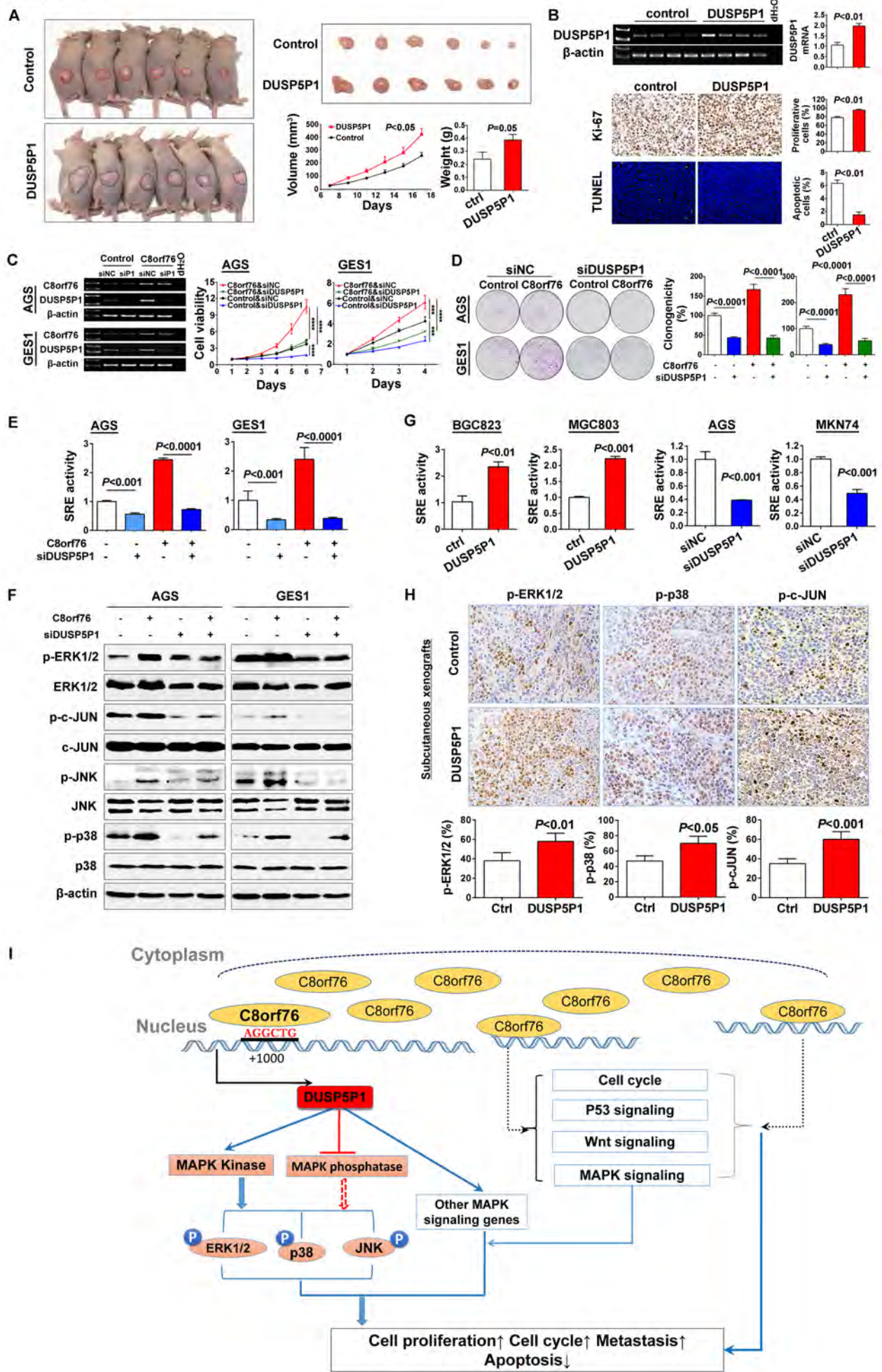


Figure 6



Clinical Cancer Research

C8orf76 promotes gastric tumorigenicity and metastasis by directly inducing lncRNA DUSP5P1 and associates with patient outcomes

Xiaohong Wang, Jessie QY Liang, Lian-Hai Zhang, et al.

Clin Cancer Res Published OnlineFirst February 7, 2019.

Updated version	Access the most recent version of this article at: doi: 10.1158/1078-0432.CCR-18-2804
Supplementary Material	Access the most recent supplemental material at: http://clincancerres.aacrjournals.org/content/suppl/2019/02/08/1078-0432.CCR-18-2804.DC1
Author Manuscript	Author manuscripts have been peer reviewed and accepted for publication but have not yet been edited.

E-mail alerts	Sign up to receive free email-alerts related to this article or journal.
Reprints and Subscriptions	To order reprints of this article or to subscribe to the journal, contact the AACR Publications Department at pubs@aacr.org .
Permissions	To request permission to re-use all or part of this article, use this link http://clincancerres.aacrjournals.org/content/early/2019/02/07/1078-0432.CCR-18-2804 . Click on "Request Permissions" which will take you to the Copyright Clearance Center's (CCC) Rightslink site.